Electronic structure of linear TiCH

Apostolos Kalemos and Thom H. Dunning, Jr.[a)]
Joint Institute for Computational Science, University of Tennessee—Oak Ridge National Laboratory, Oak Ridge, Tennessee 37831-6414

James F. Harrison
Department of Chemistry and Center for Fundamental Materials Research, Michigan State University, East Lansing, Michigan 48824-1322

Aristides Mavridis
National and Kapodistrian University of Athens, Department of Chemistry, Laboratory of Physical Chemistry, PO Box 64004, 157 10 Zografou, Athens, Greece

(Received 26 February 2003; accepted 29 April 2003)

The linear TiCH molecule is studied by *ab initio* quantum mechanical calculations using quantitative basis sets and highly correlated computational methods. Potential energy curves along the Ti−CH coordinate have been computed to obtain a better understanding of molecular formation in eight low-lying states of the molecule. Total energies, dissociation energies (with respect to Ti +CH), equilibrium distances, and dipole moments are reported. Simple valence bond Lewis diagrams are used to interpret the nature of the bonding in all of the states studied. © *2003 American Institute of Physics.* [DOI: 10.1063/1.1584425]

I. INTRODUCTION

Transition metal compounds are conceptually interesting and technologically important. In particular, the importance of transition metals in catalysis, which is caused in part by the high density of low-lying states of the participating metal atom(s), is well recognized. Modern electronic structure theory is one of the best approaches for obtaining a detailed understanding of these complex systems.[1] Despite the tremendous progress of the last 30 years in *ab initio* all-electron quantum mechanical calculations, quantitative predictions are still not easily made even for the simplest diatomic MX[2] or triatomic MXY molecular systems, where M is a first row transition metal atom and (X, Y) are main group elements. The fundamental difficulty of accurately solving the nonrelativistic Schrödinger equation for such systems is due, mainly, to the aforementioned multitude of low-lying states of the M atoms or cations (M^+) coupled with significant differential electron correlation effects among the states.

In the current paper, we investigate one of the isomers of the triatomic molecule titanium methylidyne, TiCH. TiCH is one of the simplest organometallic systems, which, nevertheless, can be used as a stepping stone to the study of more complex molecules. In addition, some recent experimental findings obtained by laser-induced fluorescence spectroscopy are available for the Ti−CH molecule.[3] Although experimental results on the $\tilde{X}\,^2\Sigma^+$ state are limited, namely,

$$r_0(\mathrm{Ti-CH}) = 1.7277 \pm 0.0003 \ \text{Å},$$

$$r_0(\mathrm{TiC-H}) = 1.085 \pm 0.002 \ \text{Å},$$

and

$$\nu_2(\text{bend}) = 578 \ \mathrm{cm}^{-1},$$

$$\nu_3(\text{Ti-C stretch}) = 855 \ \mathrm{cm}^{-1},$$

they are valuable benchmarks for the present theoretical study.

We can consider the linear TiCH molecule to be formed from the interaction Ti+CH or TiC+H. These asymptotic fragments are essentially isoenergetic, because the ground state binding energies of C−H[4] and Ti−C,[2(b)] 83.7 and 82.3 kcal/mol, respectively, are nearly equivalent. We can visualize the Ti+CH and TiC+H interactions by using simple valence bond Lewis (vbL) diagrams, taking into account the lowest states of the fragments.

The electronic structure of the ground states of Ti($4s^2 3d^2; a^3$F) and CH($X^2\Pi$) is not expected to give rise to a strong attractive interaction in the linear configuration. However, a ''triple'' bond can be naturally formed from the interaction of the first excited states of Ti($4s^1 3d^3; a^5$F) and CH($a^4\Sigma^-$), which are just 18.6 (Ref. 5) and 17.2 kcal/mol[4] above their ground states, respectively. This results in linear $^2\Sigma^+$ or $^2\Delta$ states. The following vbL diagram represents these configurations:

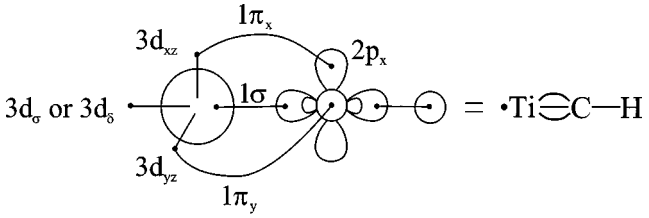

(1)

It is worth noting that the CH fragment is isoelectronic with nitrogen and its $a^4\Sigma^-$ state is ''isovalent'' with N(^{4}S). In-

a)Author to whom correspondence should be addressed. Electronic mail: dunning@jics.utk.edu

deed, the ground state of TiN is $^2\Sigma^+$ with a binding energy of $D_e=99.6$ kcal/mol at $r_e=1.613$ Å, as obtained at the multireference level.[6]

The ground state of TiC is of $^3\Sigma^+$ symmetry with the first excited state ($a^1\Sigma^+$) just 1.55 kcal/mol higher at the multireference configuration interaction level.[2(b)] The next states of TiC of $^3\Delta$ and $^1\Delta$ symmetry are 18.8 and 23.7, kcal/mol higher,[2(b)] and therefore they will not be considered further. From the vbL diagram of the $^{1,3}\Sigma^+$ states of TiC

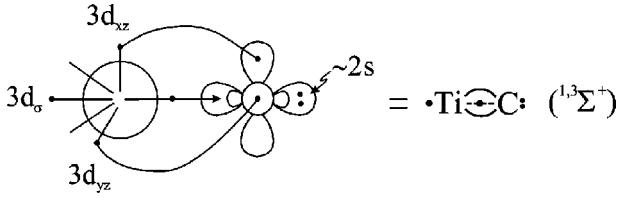

$$\mathrm{Ti}(a^5\mathrm{F};\ \mathrm{M}=0)\quad \mathrm{C}(^3\mathrm{P};\ \mathrm{M}=0) \tag{2}$$

it is clear that the formation of the Ti−CH isomer arising from the interaction of the H(^{2}S) atom with TiC($X^3\Sigma^+$) from the carbon-end requires excitation of the *in situ* C atom. The natural approach would be from the Ti-end, resulting in the formation of the linear H−Ti−C($^2\Sigma^+$) isomer.

The above discussion clearly suggests that the ground state of TiCH is linear with a ground state of $^2\Sigma^+$ or $^2\Delta$ symmetry. Indeed, our calculations confirm, in agreement with the experimental results,[3] that the $^2\Sigma^+$ state is the ground state.

The interaction of Ti(a^3F,a^5F)+CH($X^2\Pi$,$a^4\Sigma^-$) gives rise to the following molecular states:

$$\mathrm{Ti}(4s^23d^2;a^3\mathrm{F})+\mathrm{CH}(X^2\Pi)$$
$$=^{2,4}\{\Sigma^\pm,\Pi(2),\Delta(2),\Phi,\Gamma\},$$
$$\mathrm{Ti}(4s^23d^2;a^3\mathrm{F})+\mathrm{CH}(a^4\Sigma^-)$$
$$=^{2,4,6}\{\Sigma^\pm,\Pi,\Delta,\Phi\},$$
$$\mathrm{Ti}(4s^13d^3;a^5\mathrm{F})+\mathrm{CH}(X^2\Pi)$$
$$=^{4,6}\{\Sigma^\pm,\Pi(2),\Delta(2),\Phi,\Gamma\},$$
$$\mathrm{Ti}(4s^13d^3;a^5\mathrm{F})+\mathrm{CH}(a^4\Sigma^-)=^{2,4,6,8}\{\Sigma^\pm,\Pi,\Delta,\Phi\}.$$

In the current article, we report potential energy curves for nine (9) Ti+CH states of symmetry $(\tilde{X})^2\Sigma^+$, $^{2,4}\Pi$, $^{2,4}\Delta(2)$, and $^{2,4}\Phi$. Multireference configuration interaction methods in conjunction with quantitative basis sets (*vide infra*) are employed. All calculated states correlate adiabatically to the ground state fragments, Ti(a^3F)+CH($X^2\Pi$).

II. METHODOLOGICAL DETAILS

For the Ti atom we use the ANO ($21s16p9d6f4g$) basis set of Bauschlicher contracted to $[7s6p4d3f2g]$.[7] For the C and H atoms the correlation consistent basis sets of quadruple and triple zeta quality, respectively, were employed: C($12s6p3d2f1g$) contracted to C$[5s4p3d2f1g]$ and H($5s2p1d$) contracted to H$[3s2p1d]$.[8] The total one-electron space contains 153 spherical Gaussian functions.

Potential curves were constructed at the complete active space-self consistent field+single+double replacements (CASSCF+1+2=MRCI) level. Close to the equilibrium internuclear separations, the $\tilde{X}\,^2\Sigma^+$ and the first $^2\Delta$ states were also calculated using the restricted singles and doubles coupled cluster method (CCSD) with a perturbative correction for triples, i.e., the RCCSD(T) method.[9]

The zeroth "valence" space contains 12 orbitals correlating to the valence space of the three atoms Ti($4s+4p_z+3d$)+C($2s+2p$)+H($1s$). By distributing the nine active (valence) electrons in 12 orbitals, the CAS zeroth order wave functions range from 3700 to 48 000 configuration functions (CFs), according to the spatial-spin symmetry of the state. Symmetry and equivalence restrictions were imposed on the orbitals in the CASSCF wave function. For the construction of the potential energy curves, stated-averaged CASSCF orbitals were used. For the geometry optimizations, CASSCF wave functions were individually optimized for all but the two $^4\Delta$ states.

Keeping the $1s^22s^22p^63s^23p^6$ configuration of Ti and $1s^2$ configuration of carbon always fully occupied, the size of the contracted MRCI wave functions consists of about 6×10^6 CFs. Because the Ti($3s$,$3p$) orbitals are of nearly the same spatial extent as the Ti($3d$) orbitals, freezing the Ti($3s^23p^6$) configuration will introduce an error in the calculated relative energies of the states of the Ti atom and TiCH molecule. This will be investigated in later studies.

The choice of our reference spaces ensures proper description of the fragments at infinity, i.e., our computational approach is size-consistent but with a size-extensivity error of 6.8 (2.9) millihartree at the MRCI(+Q) level of theory.

For all calculations the MOLPRO 2002.3 package was used.[10]

III. THE FRAGMENTS (Ti, CH)

Table I collects the total energies of the ground and selected excited states of the Ti atom that are involved in the formation of TiCH, along with the atomic energy separations with respect to the a^3F($4s^23d^2$) ground state. For the CH molecular fragment we report results on the ground ($X^2\Pi$) state and its first excited ($a^4\Sigma^-$) state, the latter being the *in situ* fragment of all of the molecular TiCH states presently studied. Although the CH moiety is well described by the electronic structure method/basis set chosen (see also Ref. 4), the Ti atomic separations show a significant discrepancy from the experimental values,[5] ranging from 3.1 (2.6) to 5.5 (4.5) kcal/mol at the MRCI(+Q) level of theory. These errors are due to a number of approximations invoked in the current study, especially truncation of the basis set, requiring double occupancy of the $3s$ and $3p$ core orbitals, and neglect of scalar relativistic effects.

IV. RESULTS AND DISCUSSION

In what follows we first examine the ground, $\tilde{X}\,^2\Sigma^+$, state of TiCH along with the first excited state, the $\tilde{A}\,^2\Delta$ state. We then examine the quartet and doublet states of Π and Φ symmetry and, finally, two states of $^4\Delta$ symmetry. Our numerical results, i.e., total energies (E), equilibrium geometries r_e(Ti−CH) and r_e(TiC−H), bond dissociation ener-

gies D_e(Ti−CH), dipole moments (μ) calculated as expectation values, and energy separations (T_e) with respect to the ground $\tilde{X}\,^2\Sigma^+$ state, are collected in Table II. Figure 1 is a plot of the potential energy curves (PECs) for all of these states along the Ti+CH coordinate. For all states the PECs have been constructed by keeping the TiC−H bond length at the r_e value (=1.089 Å) for the $a^4\Sigma^-$ state of CH (Table I).

A. $\tilde{X}^2\Sigma^+$, $\tilde{A}^2\Delta$ states

The ground $\tilde{X}\,^2\Sigma^+$ state correlates adiabatically to Ti(a^3F; $M_L=\pm1$)+CH($X^2\Pi$). The most important configurations at r_e are:

$$|\tilde{X}\,^2\Sigma^+\rangle \approx |1\sigma^2 2\sigma^2 3\sigma^1[0.91(1\pi_x^2 1\pi_y^2) - 0.17(2\pi_x^2 1\pi_y^2 + 1\pi_x^2 2\pi_y^2)]\rangle ,$$

where the orbital numbering refers to the active electrons only. So, the CASSCF wave function is dominated by a single reference function. The Mulliken population analysis (Ti/C/H)

$$4s^{0.84}4p_z^{0.23}3d_{z^2}^{0.50}3d_{xz}^{0.97}4p_x^{0.04}3d_{yz}^{0.97}4p_y^{0.04}/ 2s^{1.43}2p_z^{1.0}2p_x^{0.96}2p_y^{0.96}/1s^{0.95}$$

reveals the excited *in situ* character of both the Ti and CH fragments. The CH moiety is in the $a^4\Sigma^-$ state, 16.4 kcal/mol higher than its ground state at the MRCI level of theory (Table I), while the $4s^{1.0}3d_{z^2}^{1.0}3d_{xz}^{1.0}3d_{yz}^{1.0}$ configuration of the Ti atom is a mixture of the $|a^5\mathrm{F}(4s^1 3d^3);\ M_L=0\rangle$ and $|a^5\mathrm{P}(4s^1 3d^3);\ M_L=0\rangle$ spectroscopic terms, 0.942 (0.920) eV and 1.954 (1.910) eV higher than the ground Ti(a^3F) state at the MRCI(+Q) level of theory (Table I). The triple bond (scheme 1) between the Ti and CH moieties is primarily due to the low-lying $a^4\Sigma^-$ state of CH, while the absence of such electronic character in the TiC $X^3\Sigma^+$ state is due to the large energy gap[5] of the isomorphic carbon ^{5}S state, $\Delta E(^5\mathrm{S}\leftarrow a^3\mathrm{P})=96.4$ kcal/mol.[5]

From Table II we see that the binding energy of the $\tilde{X}\,^2\Sigma^+$ state with respect to Ti(a^3F)+CH($X^2\Pi$) is $D_e=104.8$ (100.1) kcal/mol at $r_e=1.742$ (1.735) Å at the MRCI(RCCSD(T)) level, the latter being 0.014 (0.008) Å longer than the experimental internuclear distance.[3] Core-correlation effects can be estimated by considering our results on TiC$^+$($X^2\Sigma^+$), where it was found that the inclusion of the $3s^2 3p^6$ Ti core electrons in the MRCI calculation increases D_e by about 4.5 kcal/mol while decreasing the bond distance by more than 0.02 Å.[2(d)] Therefore, our best estimates for D_e and r_e are 110 kcal/mol and 1.72 Å, respectively. It is interesting to note that in the Ti−CH$^+$($\tilde{X}\,^1\Sigma^+$) state at the GVB+1+2/Ti[5s4p3d]+C[3s2p1d]+H[2s1p] level,[11] the corresponding D_e and r_e values are 95.9 kcal/mol and 1.758 Å, respectively, showing the similar electronic character of the two species.

At the MRCI level the dipole moment (μ) is 1.965 D (expectation value) as opposed to 2.506 D (finite field method), reflecting mostly missing valence correlation ef-

TABLE I. Energies E (hartree) of the Ti a^3F($4s^2 3d^2$), a^5F($4s^1 3d^3$), a^3P($4s^2 3d^2$), and a^5P($4s^1 3d^3$) atomic states and corresponding energy splittings ΔE (eV), and of the CH ($X^2\Pi$ and $a^4\Sigma^-$) molecular states along with their equilibrium geometry r_e (Å) and energy gaps T_e (kcal/mol) in different methodologies.

Ti

Method	a^3F($4s^2 3d^2$)	a^5F($4s^1 3d^3$)	a^3P($4s^2 3d^2$)	a^5P($4s^1 3d^3$)	a^5F←a^3F	a^3P←a^3F	a^5P←a^3F
sa-SCF[a]	−848.405 776	−848.385 871	−848.348 214	−848.337 913	0.542	1.566	1.847
CISD	−848.460 215	−848.428 050	−848.414 332	−848.390 165	0.875	1.249	1.906
CISD+Q	−848.465 1	−848.429 4	−848.423 9	−848.392 5	0.971	1.121	1.976
sa-CASSCF[a,b]	−848.437 374	−848.386 781	−848.382 287	−848.340 676	1.377	1.499	2.631
MRCI[c]	−848.463 256	−848.428 635	−848.420 337	−848.391 439	0.942	1.168	1.954
MRCI+Q[d]	−848.463 8	−848.430 0	−848.421 8	−848.393 6	0.920	1.143	1.910
Expt.[e]					0.806	1.032	1.715

CH

State	Method	E	r_e	T_e
$X^2\Pi$	CASSCF[f]	−38.314 375	1.137	0.0
	MRCI	−38.415 159	1.122	0.0
	MRCI+Q[d]	−38.419 4	1.122	0.0
	RCCSD(T)	−38.417 522	1.121	0.0
	Expt.[g]		1.119 786	0.0
$a^4\Sigma^-$	CASSCF[f]	−38.307 651	1.091	4.22
	MRCI	−38.389 002	1.089	16.41
	MRCI+Q[d]	−38.391 7	1.090	17.42
	RCCSD(T)	−38.391 2	1.090	16.52
	Expt.[h]		[1.0977]	[17.11±0.18]

[a]Spherical average SCF or CASSCF.
[b]The active space of the CASSCF wave function contains the $4s+4p+3d$ orbitals.
[c]Valence MR-CISD wave function.
[d]+Q refers to the multireference analog of the Davidson correction.
[e]Experimental values averaged over M_J, Ref. 5.
[f]The active space of the CASSCF wave function contains the $(2s+2p)_C+(1s)_H$ orbitals.
[g]See Ref. 4.
[h]The numbers correspond to r_0 and T_0 values; see Ref. 4.

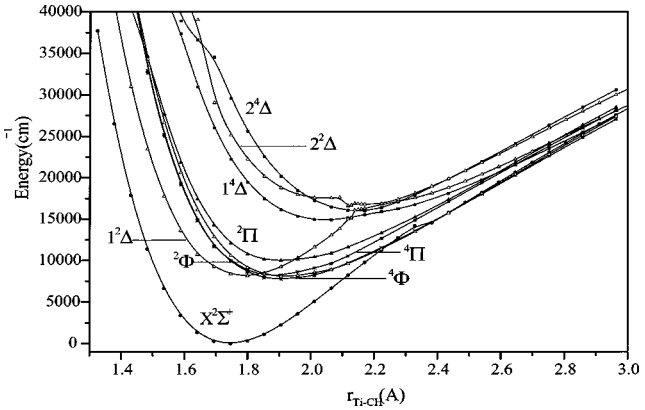

FIG. 1. Potential energy curves of the linear Ti−CH molecule at the MRCI level of theory. The r(CH) bond distance fixed at the equilibrium $a\,^4\Sigma^-$ value of CH.

fects. The nature of this difference is discussed in Ref. 12.

Considering the $X^3\Sigma^+$ state of TiC (scheme 2), the $H(^2S)+TiC(X^3\Sigma^+)$ reaction should yield the H−TiC($^2\Sigma^+$) isomer in a barrierless process. In that form the TiC fragment is not excited as the same fragment is in the Ti≡C−H case and the former species (H−TiC) is not as stable as the latter (Ti≡C−H). Indeed, the present study reveals an energy difference of 40.4 (40.5) kcal/mol at the MRCI(+Q) level of theory between the two forms. The equilibrium distances in HTiC are r_e(H−TiC)=1.882 Å and r_e(HTi−C)=1.723 Å at the MRCI level. It is interesting to note that the equilibrium distance in the TiC($X^3\Sigma^+$) species, r_e=1.712Å,[2(b)] is practically the same as in the HTiC($^2\Sigma^+$) molecule, suggesting that the electronic structure of the TiC fragment stays essentially intact upon bonding with the H(^{2}S) atom. The dipole moment is practically quenched in the HTiC($^2\Sigma^+$) case (μ=0.24 D).

The first excited state, $\tilde{A}\,^2\Delta$, retains the triple bond but the overall symmetry changes from Σ^+ to $\Lambda=2$. Its electronic character is mirrored by both the CASSCF equilibrium configurations ($^2A_1$ symmetry)

$$|1^2\Delta\rangle \approx |1\sigma^2 2\sigma^2 1\delta_+^1[0.91(1\pi_x^2 1\pi_y^2) - 0.19(2\pi_x^2 1\pi_y^2 + 1\pi_x^2 2\pi_y^2)]\rangle$$

and its Mulliken atomic distributions:

$$4s^{0.25}4p_z^{0.05}3d_{z^2}^{0.34}3d_{xz}^{0.89}4p_x^{0.05}3d_{yz}^{0.89}4p_y^{0.05}3d_{x^2-y^2}^{1.0}/$$
$$2s^{1.41}2p_z^{0.94}2p_x^{1.04}2p_y^{1.04}/1s^{0.98}.$$

Although the Ti(a^5F; $M_L=\pm 2$) component, which is responsible for the bonding in the present state, is not a mixture with the a^5P state as in the $\tilde{X}\,^2\Sigma^+$ state, the $\tilde{A}^2\Delta$ lies 20.9 kcal/mol higher than the ground state (Table II), suggesting that the σ electron in the $\tilde{X}\,^2\Sigma^+$ state contributes to the stabilization of this state whereas the δ electron does not play such a role in the $\tilde{A}\,^2\Delta$ state.

From Table II we see that the dipole moment of the $\tilde{A}\,^2\Delta$ state is exceptionally high, 7.24 D, as contrasted to 1.96 D in the $\tilde{X}\,^2\Sigma^+$ state. In both states ($\tilde{X}\,^2\Sigma^+$ and $\tilde{A}\,^2\Delta$) TiCH has a high ionic contribution with a positive charge of 0.4–0.5

TABLE II. Total energies E (hartree), dissociation energies D_e (kcal/mol), bond distances r_e(Ti-CH), r_e(TiC-H) (Å), dipole moments μ (D), and energy gaps T_e (kcal/mol) of the calculated states of TiCH.

State	Method	E	D_e	r_e(Ti-CH)	r_e(TiC-H)	μ	T_e
$\tilde{X}^2\Sigma^+$	MRCI	−887.036 569	104.8	1.742	1.093	1.96 (2.51)[b]	0.0
	MRCI+Q	−887.045 1	103.1				0.0
	RCCSD(T)	−887.041 766	100.1	1.735	1.093		0.0
	Expt.[a]			1.7277±0.0003	1.085±0.002		0.0
$\tilde{A}\,^2\Delta$	MRCI	−887.003 203	83.9	1.792	1.095	7.24	20.9
	MRCI+Q	−887.014 7	84.1				19.0
	RCCSD(T)	−887.013 364	82.3	1.785	1.096		17.8
$^4\Phi$	MRCI	−887.002 693	83.5	1.894	1.092	1.35	21.3
	MRCI+Q	−887.013 1	83.0				20.1
$^4\Pi$	MRCI	−887.001 337	82.7	1.879	1.093	1.55	22.1
	MRCI+Q	−887.012 2	82.4				20.7
$^2\Phi$	MRCI	−887.001 282	82.7	1.912	1.091	1.30	22.1
	MRCI+Q	−887.011 4	82.0				21.1
$^2\Pi$	MRCI	−886.992 246	77.0	1.895	1.091	1.31	27.8
	MRCI+Q	−887.003 4	76.9				24.1
$^4\Delta(1)$	MRCI	−886.968 519	62.1	2.049	1.092	0.05	42.7
	MRCI+Q	−886.979 5	62.0				41.2
$^4\Delta(2)$	MRCI	−886.964 504	59.6	2.172	1.096	0.23	45.2
	MRCI+Q	−886.971 7	57.0				46.1

[a]Experimental results refer to r_0 values, Ref. 3.
[b]This value has been calculated using the finite field approach.

on Ti and a corresponding excess of electrons on the C atom. In the $\tilde{A}$-case a localized δ electron on the metal atom creates a rather large dipole moment while in the $\tilde{X}$-case the σ electron responsible for both the spatial and spin symmetry, $\sim 0.61(4s) - 0.25(3d_{z^2}) - 0.43(4p_z)$, counterbalances the negative C region and drastically reduces the dipole moment.

B. $^4\Phi$, $^4\Pi$, $^2\Phi$, and $^2\Pi$ states

All of these states correlate adiabatically to $\mathrm{Ti}(a^3\mathrm{F};\ M_L = \pm 2) + \mathrm{CH}(X^2\Pi)$, with bonding similarities around equilibrium. In each of these states there is a double bond between the Ti and C atoms and three unpaired electrons that couple into doublet and quartet symmetries. The atomic distributions of the $^4\Phi$ state at infinity

$$4s^{1.91}4p_z^{0.09}3d_{z^2}^{1.0}3d_{x^2-y^2}^{0.50}3d_{xy}^{0.50}/2s^{1.79}2p_z^{1.21}2p_x^{0.52}2p_y^{0.52}/1s^{0.90}$$

are characteristic of the $(a^3\mathrm{F};\ M_L = \pm 2) \otimes (X^2\Pi)$ configurations as dictated by symmetry, while at equilibrium

$$4s^{0.84}4p_z^{0.32}3d_{z^2}^{0.28}3d_{xz}^{0.56}4p_x^{0.03}3d_{yz}^{0.56}4p_y^{0.03}3d_{x^2-y^2}^{0.50}3d_{xy}^{0.50}/$$
$$2s^{1.48}2p_z^{1.09}2p_x^{0.89}2p_y^{0.89}/1s^{0.93}$$

reveals the *in situ* excited character of the parental species $\mathrm{Ti}(a^3\mathrm{F};\ M_L = \pm 2 \rightarrow a^5\mathrm{F};\ M_L = \pm 3)$ and $\mathrm{CH}(X^2\Pi \rightarrow a^4\Sigma^-)$. The CASSCF equilibrium configurations

$$\begin{aligned}|^4\Phi\rangle \approx 0.64[&|1\sigma^2 2\sigma^2 3\sigma^1 1\pi_x^2 1\pi_y^1 1\delta_-^1\rangle \\ &+ |1\sigma^2 2\sigma^2 3\sigma^1 1\delta_+^1 1\pi_x^1 1\pi_y^2\rangle] \\ &- 0.14[|1\sigma^2 2\sigma^2 3\sigma^1 2\pi_x^2 1\pi_y^1 1\delta_-^1\rangle \\ &+ |1\sigma^2 2\sigma^2 3\sigma^1 1\delta_+^1 1\pi_x^1 2\pi_y^2\rangle]\end{aligned}$$

are in agreement with the above mentioned electronic character change and graphically presented by the following vbL diagram

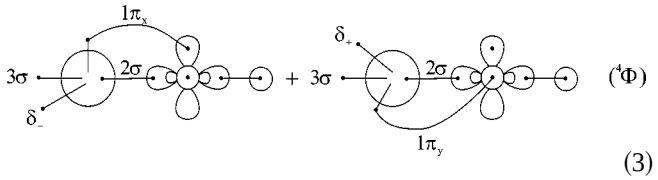

(3)

Therefore, the $^4\Phi$ state is formally described as a (σ,π)-bonded system.

The $^4\Pi$ state is in every respect similar to the $^4\Phi$ state (Table II) with the same equilibrium atomic distributions and CASSCF configurations. The only difference, as dictated by the spatial $|\Lambda| = 1$ symmetry, is a sign change ("$-$" instead of a "$+$") to the $^4\Phi$ expression and vbL diagram.

The $^2\Phi$ and $^2\Pi$ states are analogous to the $^4\Phi$ and $^4\Pi$ states, respectively. The electronic characteristics remain intact with a recoupling of the spins of the electrons in the open σ, π, and δ orbitals. Experimentally,[3] a $^2\Pi \leftarrow \tilde{X}\,^2\Sigma^+$ transition is observed in the range 13 815–15 080 cm^{-1}. The $^2\Pi$ state found in the current work lies just 27.8 kcal/mol ($=9728\ \mathrm{cm}^{-1}$) higher than the $\tilde{X}$-state at the MRCI level of theory (12 098 cm^{-1} higher for the vertical transition energy). Further, the substantial change in the r_e of the $\tilde{X}$ and $^2\Pi$ states suggests a broad band for the $^2\Pi \leftarrow \tilde{X}\,^2\Sigma^+$ transition. Thus, it appears that the $^2\Pi$ state studied here is not the one observed experimentally. Previous work[13] suggests that in the experimentally observed $^2\Pi$ state the TiC triple bond is preserved and the π electron is in a Ti $4p$ orbital. We were unable to calculate a higher $^2\Pi$ state because of technical problems (convergence problems in the CASSCF calculations as well as root flipping problems in the MRCI calculations). It is also likely that titanium $4p_{x,y}$ orbitals would need to be included in the CASSCF calculations to properly describe the experimentally observed $^2\Pi$ state; this was not feasible in the current work.

C. $^4\Delta(1)$ and $^4\Delta(2)$ states

The asymptotic character of both $^4\Delta$ states is described by the $|a^3\mathrm{F},\ M_L = \pm 3, \pm 1\rangle_{\mathrm{Ti}} \otimes |X^2\Pi\rangle_{\mathrm{CH}}$ product with corresponding atomic distributions of

$$4s^{1.90}4p_z^{0.10}3d_{xz}^{0.50}3d_{yz}^{0.50}3d_{x^2-y^2}^{0.50}3d_{xy}^{0.50}/$$
$$2s^{1.79}2p_z^{1.22}2p_x^{0.52}2p_y^{0.52}/1s^{0.90}\ \ (^4\Delta(1))$$

and

$$4s^{1.90}4p_z^{0.09}3d_{z^2}^{0.38}3d_{xz}^{0.50}3d_{yz}^{0.50}3d_{x^2-y^2}^{0.31}3d_{xy}^{0.31}/$$
$$2s^{1.79}2p_z^{1.22}2p_x^{0.52}2p_y^{0.52}/1s^{0.90}\ \ (^4\Delta(2)).$$

The equilibrium molecular distribution is dictated by the excited CH fragment; the Ti atom should consequently adjust itself in order to carry the $|\Lambda| = 2$ symmetry. The equilibrium configurations and population analysis for both states are

$$\begin{aligned}|^4\Delta(1)\rangle \approx 0.80&|1\sigma^2 2\sigma^2 3\sigma^2 1\pi_x^1 1\pi_y^1 1\delta^1\rangle \\ &- 0.32|1\sigma^2 2\sigma^2 4\sigma^2 1\pi_x^1 1\pi_y^1 1\delta^1\rangle \\ &- 0.34|1\sigma^2 2\sigma^2 3\sigma^1 4\sigma^1 1\pi_x^1 1\pi_y^1 1\bar{\delta}^1\rangle \\ &- 0.12|1\sigma^2 2\sigma^2 3\sigma^1 4\sigma^1 1\bar{\pi}_x^1 1\pi_y^1 1\delta^1\rangle\end{aligned}$$

$$4s^{1.07}4p_z^{0.42}3d_{z^2}^{0.95}3d_{xz}^{0.07}4p_x^{0.04}3d_{yz}^{0.07}4p_y^{0.04}3d_{\delta}^{1.0}/$$
$$2s^{1.48}2p_z^{1.13}2p_x^{0.87}2p_y^{0.87}/1s^{0.91}$$

and

$$\begin{aligned}|^4\Delta(2)\rangle \approx 0.70&|1\sigma^2 2\sigma^2 3\sigma^1 4\sigma^1 1\bar{\pi}_x^1 1\pi_y^1 1\delta^1\rangle \\ &+ 0.49|1\sigma^2 2\sigma^2 3\sigma^1 4\sigma^1 1\pi_x^1 1\bar{\pi}_y^1 1\delta^1\rangle \\ &- 0.22|1\sigma^2 2\sigma^2 3\sigma^1 4\sigma^1 1\pi_x^1 1\pi_y^1 1\bar{\delta}^1\rangle\end{aligned}$$

$$4s^{0.89}4p_z^{0.54}3d_{z^2}^{1.01}3d_{xz}^{0.06}4p_x^{0.03}3d_{yz}^{0.06}4p_y^{0.03}3d_{\delta}^{1.0}/$$
$$2s^{1.49}2p_z^{1.10}2p_x^{0.89}2p_y^{0.89}/1s^{0.91}.$$

The Mulliken atomic distributions reveal an excited Ti atom which cannot be of $4s^1 3d^3$ configuration since the $M_L = \pm 2$ component of such distribution is of $4s^{1.0}3d_{xz}^{1.0}3d_{yz}^{1.0}3d_{\delta}^{1.0}$, inconsistent with the present data. The Ti atom should be in a $4s^{1.0}4p_z^{1.0}3d_{z^2}^{1.0}3d_{\delta}^{1.0}$ ($4s^1 4p^1 3d^2$, $^5\mathrm{G}$; $M_L = \pm 2$) state giving rise to the follow-

ing situation schematically described by

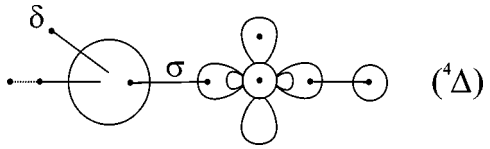

(4)

The T_e energy values of both states (Table II), 42.7[$^4\Delta(1)$] and 45.2[$^4\Delta(2)$] kcal/mol, are in harmony with this highly excited Ti state to which these molecular states correlate diabatically.

V. SYNOPSIS AND REMARKS

We have studied eight molecular states, $\tilde{X}\,^2\Sigma^+$, $^2\Delta$, $^{2,4}\Phi$, $^{2,4}\Pi$, and $^4\Delta(1,2)$, of the linear TiCH molecule mainly by MRCI methods and nearly quantitative basis sets. All states dissociate adiabatically to the ground states of Ti(a^3F) and CH($X^2\Pi$), but at equilibrium the fragment configurations are best represented by the excited states Ti(a^5F) + CH($a^4\Sigma^-$), as evidenced by the electronic character of the *in situ* fragments. For all states we report potential curves, bond distances, dissociation energies, and dipole moments. For two states, $\tilde{X}\,^2\Sigma^+$ and $\tilde{A}\,^2\Delta$, we also report D_e and r_e values at the RCCSD(T) level of theory.

It is found that the ground state is of $^2\Sigma^+$ symmetry in accord with recent experimental results.[3] At the MRCI level the binding energies for the states studied range from 105 ($\tilde{X}\,^2\Sigma^+$) to 57 ($^4\Delta(2)$) kcal/mol with respect to ground state fragments Ti+CH. Taking as a benchmark the results on $TiC^+(X^2\Sigma^+)$,[2(d)] it is reasonable to suggest an increase by about 4–5 kcal/mol in the D_e values and a decrease of 0.02 Å in the r_e(Ti−CH) values for all states. The D_e and r_e results on the $\tilde{X}\,^2\Sigma^+$ and $\tilde{A}\,^2\Delta$ states obtained using the RCCSD(T) approach are very similar to those from the corresponding MRCI calculations reflecting the strong single reference character of these states.

The first excited state, $\tilde{A}^2\Delta$, is located 20.9 (17.8) kcal/mol above the $X^2\Sigma^+$ state at the MRCI(RCCSD(T)) level, but four states, namely $\tilde{A}\,^2\Delta$, $^4\Phi$, $^4\Pi$, and $^2\Phi$, are practically degenerate within the accuracy of our calculations. The lowest $^2\Pi$ state is characterized by a TiC double bond as opposed to the experimentally observed $^2\Pi$ state which most likely has a triple bond and is higher in energy. Note that we report T_e values as opposed to T_0 values, because of technical problems in obtaining the harmonic frequencies.

Finally we would like to mention that for all states and within interatomic Ti−CH distances of 9–10 bohr van der Waals interactions in the range 20 to 140 cm^{-1} were calculated.

[1] See, for instance, E. R. Davidson, Chem. Rev. **100**, 351 (2000).
[2] (a) A. Kalemos, A. Mavridis, and J. F. Harrison, J. Phys. Chem. A **105**, 755 (2001); (b) A. Kalemos and A. Mavridis, *ibid.* **106**, 3905 (2002); (c) D. Tzeli and A. Mavridis, J. Chem. Phys. **116**, 4901 (2002); (d) I. S. K. Kerkines and A. Mavridis, Collect. Czech. Chem. Commun. **68**, 387 (2003).
[3] M. Barnes, A. J. Merer, and G. F. Metha, J. Mol. Spectrosc. **181**, 168 (1997).
[4] A. Kalemos, A. Mavridis, and A. Metropoulos, J. Chem. Phys. **111**, 9536 (1999).
[5] C. E. Moore, Atomic Energy Levels, NSRDS-NBS Circular 3 (U.S. GPO Washington, D.C., 1971).
[6] J. F. Harrison, J. Phys. Chem. **100**, 3513 (1996).
[7] C. W. Bauschlicher, Jr., Theor. Chim. Acta **92**, 183 (1995).
[8] T. H. Dunning, Jr., J. Chem. Phys. **90**, 1007 (1989). Basis sets were obtained from the Extensible Computational Chemistry Environment Basis Set Database, Version 7/30/02, as developed and distributed by the Molecular Science Computing Facility, Environmental and Molecular Sciences Laboratory which is part of the Pacific Northwest Laboratory, P.O. Box 999, Richland, WA 99352, and funded by the U.S. Department of Energy. The Pacific Northwest Laboratory is a multi-program laboratory operated by Battelle Memorial Institute for the U.S. Department of Energy under Contract No. DE-AC06-76RLO 1830. Contact David Feller or Karen Schuchardt for further information.
[9] K. Ragavachari, G. W. Trucks, J. A. Pople, and M. Head-Gordon, Chem. Phys. Lett. **157**, 479 (1989).
[10] MOLPRO, a package of *ab initio* programs designed by H.-J. Werner and P. J. Knowles, version 2002.3, R. D. Amos, A. Bernhardsson, A. Berning *et al.*
[11] A. Mavridis, A. E. Alvarado-Swaisgood, and J. F. Harrison, J. Phys. Chem. **90**, 2584 (1986).
[12] D. Tzeli and A. Mavridis, J. Chem. Phys. **118**, 4984 (2003).
[13] E. Edwards, Ph.D. thesis, Michigan State University, 1998.